Influence of partial substitution for CB with MWNTs on performance of CB-filled NR composites

Huan Zhang[1], *Yintao Wei*[1] ✉, *Zhenran Kang*[1], *Guizhe Zhao*[2], *Yaqing Liu*[2]

[1]*The State Key Laboratory of Automotive Safety and Energy, Tsinghua University, Beijing 100084, People's Republic of China*
[2]*Shanxi Key Laboratory of Nano Functional Composite Materials, North University of China, Taiyuan 030051, People's Republic of China*
✉ *E-mail: weiyt@tsinghua.edu.cn*

Published in Micro & Nano Letters; Received on 22nd August 2016; Revised on 8th October 2016; Accepted on 17th October 2016

The effects of substituting carbon black (CB) with multiwall carbon nanotubes (MWNTs) on the structure and properties of natural rubber (NR)/CB composites is explored. Compared with NR/CB composites, NR/MWNTs/CB presents better filler dispersity and dynamic properties of the MWNT up to a certain concentration, as confirmed by scanning electron microscope, dynamic mechanical analyser and rubber processing analyser. Sample with 1 phr MWNTs shows obviously the highest tensile strength, 28.60 MPa, and almost the lowest heat build-up, only 9.6°C, and it is attributed to that not only large cross-link density and better filler dispersity but also high effective elasticity and large filler–rubber interaction. However, when the concentration is much higher, MWNTs tend to aggregate and lead to the poor efficiency to enhance the dynamic properties of rubber composites or even deteriorate the properties.

1. Introduction: Natural rubber (NR) shows plentiful excellent performance for instance low gas permeability, rolling resistance, high strength and coupled with improved wet grip; even more than synthetic rubber [1]. Although NR exhibits plentiful excellent performance, in order to gain the appropriate properties for specific applications, to add reinforcing fillers into it is necessary in most cases. For various purposes, multitudinous fillers are applied in the rubber industry and the most important purpose is reinforcement, improvements in processing and reduction in material costs [2]. The enhancement of strength-related properties such as strength, modulus, hardness and abrasion resistance is called reinforcement [3, 4]. Carbon black (CB) was the main reinforcing filler to increase the usefulness of rubber in most applications. Modulus, abrasion resistance, tear strength and tensile strength are enhanced when CB is compounded with rubbers. To decrease the dosage of fillers, the researchers use high-performance reinforcing filler, e.g. multiwalled carbon nanotubes (NTs) [5, 6], graphene oxide and graphene [7] and so on, to partially replace the CB. Multiwall carbon NTs (MWNTs) have good reinforcing effect and a high aspect ratio owing to its tubular form; thus it is a good latent reinforcing filler of rubber. However, owing to the specific structure and the high surface area of particles, MWNTs have high filler–filler interaction, and therefore they tend to form agglomerates and entanglements. Solution mixing was used in most of recent published studies owing to better dispersion [8–11]. Moreover, to improve dispersion recent, some scholars do it successfully by pretreatment of MWNTs [12, 13] and combining MWNTs with CB. Compared with the CB-filled compounds, Bokobza *et al.* [14] achieved improvements in the stress–strain properties by using blend of MWNTs with CB in styrene–butadiene rubber, owing to improved polymer–filler interaction.

Although several studies have been made to elucidate composites with MWNTs and CB, the effect of MWNTs and CB on the dynamic properties and heat build-up of vulcanisates are rarely reported. The purpose of this Letter is to explore a method to prepare NR composites with high strength, good dynamic properties and low heat build-up. Therefore, NR composites were prepared by the method which combined the modified latex co-precipitation masterbatch and mechanical blending and studied in detail. The cure characteristics, mechanical properties, morphological, heat build-up and dynamic properties of NR were investigated and discussed.

2. Experimental

2.1. Materials: The purified MWNTs used here were offered by Shenzhen Nano Port Co., Ltd. The outer diameter of MWNTs was 20–30 nm, the inner diameter was 5–10 nm and the length varied from 10 to 30 μm. NR (1# smoke sheet rubber) was provided by Hainan Agricultural Reclamation Co., Ltd. The fresh NR latex (natural latex solid content is 60%) used in this Letter was obtained from the Local state-owned Qionghai Lixin farm rubber processing factory. CB (N330) was purchased from China Rubber Group Carbon Black Research Institute. The other compound ingredients of rubber were used as received and all commercially available.

2.2. Preparation of nanocomposites: Masterbatches of MWNT with NR were prepared using by an aqueous coagulation method. Add a certain amount of MWNTs to 50 g fresh NR latex and stirred for 1 h by magnetic action, and coagulated by the addition of flocculant calcium chloride ($CaCl_2$) to produce a NR-MWNTs masterbatch. Then, NR-MWNTs masterbatch was cut into small pieces and well washed to remove $CaCl_2$, and dried at 70°C for at least 36 h to remove the water. A control NR sample was prepared by the same process but with no MWNT added.

The NR/CB/MWNTs composites are named as NR/MWNTs/CB (NM)-*x* and *x* is the mass fraction of CB replaced by MWNTs. The formulation of NM composites is listed in Table 1. Except the curatives, other ingredients were mixed with NR including NR-MWNTs masterbatch for 15 min at 110°C in a laboratory-size internal mixer. Then, the curatives were added to the compounds and mixed on a two roll-mill (Shanghai Rubber Machinery Factory, SK-160B) below 40°C. The compounds were hot-pressed and vulcanised under the pressure of 13 MPa at 150°C × T_{c90}. An M-3000A rheometer (High Speed Rail Instrument Testing Company, Taiwan, China) was used to measure the T_{c90}.

2.3. Mechanical characterisation: Tensile properties were measured by an AI-7000-SGD (Taiwan) instrument at 25°C with an initial clamp separation of 65 mm and the crosshead rate was 500 mm/min, according to international standard organisation (ISO) standard

Table 1 Composition of NM nanocomposites

Samples[a]	NM-0	NM-0.5	NM-1.0	NM-1.5	NM-2.0
NR (dry)	70	70	70	70	70
NR (latex)	30	30	30	30	30
MWNTs	0	0.5	1.0	1.5	2.0
N330	40	39.5	39	38.5	38

[a]All the samples contain the below additives: Zinc oxide (5), stearic acid (2), poly(1,2-dihydro-2,2,4-trimethyl-quinoline) (1), *N*-Isopropyl-*N*′-phenyl-4-phenylenediamin (1), *N*-(oxidiethylene)-2-benzothia-zolyl sulphenamide (2) and sulphur (2)

37-2005. According to ISO standard 7619-1997, shore A hardness was tested by an XHS-W sclerometer (Liaoning). The standard deviations for tear strength, tensile strength, hardness, modulus at 100%, 300% elongation and elongation at break are ±0.5, ±0.4, ±1, ±0.1, ±0.3 and ±5.0 units, respectively. The specimens were aged at 100°C for 22 h in a circulating air chamber to study the heat ageing resistance. Before testing, the aged samples were left at least 18 h at room temperature.

The hysteresis loss was determined using (1)

$$H_k = (W_1 - W_2)/W_1 \times 100 \tag{1}$$

where W_1, W_2 and H_k are work performed during forward deformation, reverse deformation and hysteresis loss, respectively.

The testing samples were chopped in dimensions of 90 × 6 × 2 mm, and scale distance is 10 mm. For tensile testing, the crosshead rate was 500 mm/min during forward deformation and tensile force was 1 N during reverse deformation. All samples experience four cycles. Hysteresis test was performed till tensile force to 25 N, and only reported the hysteresis loss for the fourth cycle. Meanwhile, the effective elasticity is defined as

$$\eta_k = W_2/W_1 \times 100 \tag{2}$$

2.4. Determination of cross-link density: Equilibrium swelling method was used to study the cross-link density. To remove substances such as remains of activators and accelerators, samples were initially put in acetone for 24 h in a soxhlet apparatus and then dried the samples at 50°C in a vacuum oven. The extracted samples were swollen in *n*-heptane for 48 h at room temperature, then weighed and dried in a vacuum oven to a constant weight at 50°C and weighed again. According to Flory–Rehner [15–19], the cross-link density was calculated.

2.5. Bound rubber: Compounds (without curatives) were first kept at room temperature for 7 days for conditioning, to determine the bound rubber content, then cut into small pieces and immersed in 100 ml toluene in a stainless-steel wire cage using about 0.5 g of the sample. On the fourth day, the solvent was renewed and the samples were taken out of the solvent after 7 days, and dried in vacuum at 60°C to a constant weight.

Table 2 Vulcanisation characteristics of NM compounds

MWNTs/CB ratio	T_{S2}, min	T_{c90}, min	M_H, Nm	M_L, Nm	M_H–M_L, Nm	CRI, min^{-1}
0/40	2.74	6.22	2.32	0.03	2.29	28.74
0.5/39.5	2.86	6.18	2.42	0.04	2.38	30.12
1.0/39	2.86	6.10	2.50	0.05	2.45	30.86
1.5/38.5	2.74	5.86	2.63	0.03	2.60	32.05
2.0/38	2.94	6.18	2.76	0.05	2.71	30.86

The following equation (3) was used to calculate the bound rubber percentage (R_b) [20]

$$R_b(\%) = 100 \times \frac{W_{fg} - W_t[m_f/(m_f + m_r)]}{W_t} \tag{3}$$

m_r was the weight fraction of the polymer in the original sample, m_f was the weight fraction of the filler in the gel, W_{fg} was the weight of the dried gel and W_t was the weight of the original sample.

2.6. Rubber–filler interaction: Park and Lorenz equation (4) was used to determine the rubber–filler interaction [21]

$$Q_f/Q_g = ae^{-z} + b \tag{4}$$

z is the ratio by weight of the filler to the rubber hydrocarbon in the vulcanisates, subscripts f and g are corresponding to filled and gum samples and a, b are constants, respectively. The dimension of cured sample was 30 × 5 × 2 mm. Samples were immersed in toluene at 25°C until equilibrium swelling for 48 h and then were dried until constant weights were obtained in an oven at 60°C.

Equation (5) was used to determine the toluene uptake per gram of rubber (Q)

$$Q = (W_s - W_d)/(W_o \times \varphi_{rubber}) \tag{5}$$

where φ_{rubber} is the mass fraction of the rubber in the composites, W_o is the original weight, W_d is the dried weight and W_s is the swollen weight. When the interaction between the filler and matrix is lower, the Q_f/Q_g values are higher.

2.7. Microstructure: A field-emission scanning electron microscope (SEM) (Hitachi S-4800, Japan) was used to observe the fractured surfaces of the rubber composites. The fracture surfaces were plated with a thin layer of gold before observation.

2.8. Dynamic rheological properties of composites by rubber processing analyser: Rubber processing analyser 2000 (Alpha Technologies Co., USA) was applied to analyse the processability of rubber compounds. At the test frequency of 1 Hz at 60°C, the strain amplitude was varied from 0.28 to 400%.

2.9. Heat build-up study: According to ISO 4666 RH-3000N dynamic compression heat build-up testing instrument was used to study the dynamic compression heat build-up properties. We preheated samples for 30 min at 55°C and then applied a compressive load of 245 N on the specimen of 20 Hz frequency and 4.45 mm amplitude. The testing time was 25 min and at the base increase of temperature was recorded. The same specimen as for heat build-up testing was used to evaluate dynamic compression set. The original height of the specimen was measured before heat build-up testing and left for 1 h at 25°C after testing. Equation (6) was applied to calculate the compression set

$$\text{dynamic compression set (\%)} = [(H_O - H_f)/H_0] \times 100 \tag{6}$$

where H_f is the final height [millimetres (mm)] and H_o is the original height (mm).

3. Results and discussion

3.1. Cure characteristics: Table 2 shows the cure characteristics of rubber compound. When CB is gradually replaced by MWNTs, the torque and torque difference of vulcanisates increase. The volume fraction of fillers increased with the addition of MWNTs, as MWNTs have lower density than CB, even though the total amount of fillers was kept constant. In these compounds,

doi: 10.1049/mnl.2016.0003

Table 3 Cross-link density of vulcanisates ($\times 10^{-4}$ mol/cm^3)

MWNTs/CB ratio	0/40	0.5/39.5	1.0/39	1.5/38.5	2.0/38
Cross-link density	4.28	4.59	4.81	4.68	4.33
Cross-link density (after ageing)	4.76	5.84	5.67	5.99	5.44

movability of molecular chain decrease with CB partially replaced by MWNTs, so that torque and torque difference of vulcanisates increase, on account of MWNTs has a higher reinforcement effect compared with CB.

The cure rate index (CRI) can be calculated from the relation [22]

$$\mathrm{CRI} = \frac{100}{T_{c90} - T_{s2}}$$

It was based on the difference between optimum cure time of vulcanisation T_{c90} and the scorch time T_{s2} and the measure of rate of vulcanisation. The scorch time and cure time are mildly different with CB partially replaced by MWNTs but CRI increase, as can be seen in Table 2. This maybe a result of the decrease in T_{c90} for the samples during to strong interfacial rubber–filler interaction and pre-cross-linked (physical cross-linking for the bound rubber).

As shown in Table 3, the cross-linking density of composites is not much different with CB partially replaced by MWNTs. However, all the cross-link density increases after ageing caused by post-vulcanisation.

3.2. Mechanical properties: Modulus and hardness of composites are shown in Table 4. As expected, modulus and hardness of vulcanisates increase when CB is replaced by MWNTs and increase notably after ageing. At equal amounts of filler, samples NM-1.0 and NM-1.5 exhibit the highest modulus and hardness, followed by NM-0.5 and NM-2 composites. It maybe attributed to strong rubber–filler interaction, larger filler volume fraction and better dispersity. After ageing because of the post-vulcanisation effect the hardness, cross-linking density and modulus of composites increase considerably.

Fig. 1 shows the tear strength and tensile strength of composites. The tensile strength of composites increases when the MWNTs increase. The highest tensile strength is found for NM-1.0 composites, 28.6 MPa, maybe due to better dispersity and the increased cross-link density. The tear strength for composites all reduces obviously with an increase of MWNTs. The lowest tear strength is found for NM-2.0 composites, maybe due to poor dispersity. The tear strength of NM-1.0 composites is similar to the value of NM-0.5 and NM-1.5 composites. The results infer that MWNTs are more conducive to the tensile strength of composites compared with tear strength. As we all know, there are two cross-link densities for each vulcanisates, corresponding to the best tensile strength and best tear strength of each vulcanisates. The cross-link density for the best tensile strength is larger than that of the best tear strength. In

Table 4 100%, 300% modulus and hardness of aged and unaged composites

Properties	0/40	0.5/39.5	1.0/39	1.5/38.5	2.0/38
100% modulus, MPa	2.73	2.80	3.04	3.17	2.85
300% modulus, MPa	14.14	14.50	15.84	15.64	14.86
hardness, (shore A)	63	63	64	66	64
aged					
100% modulus, MPa	3.07	3.13	3.60	3.76	3.16
300% modulus, MPa	15.64	16.42	17.38	16.85	15.31
hardness, (shore A)	64	64	66	66	64

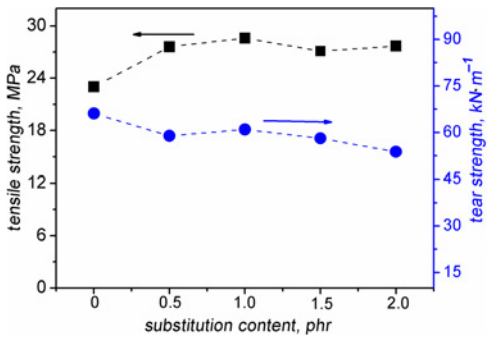

Fig. 1 *Tensile strength and tear strength of all the composites*

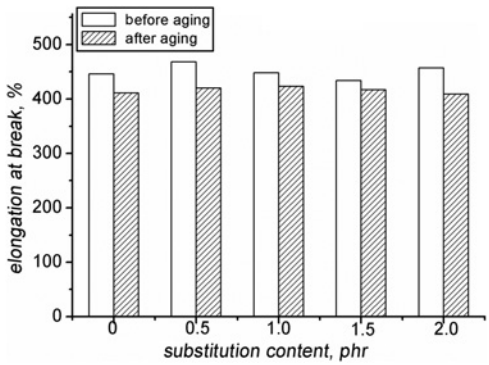

Fig. 2 *Elongation at break of all the composites*

Fig. 1, the tensile strength of composites increases when the MWNTs increase; however, the tear strength for composites all reduces obviously with an increase of MWNT. It maybe due to that the cross-link density of vulcanisates is larger than the value corresponding best tear strength.

Fig. 2 presents the elongation at break of composites. All the elongation at break of composites is superior and is not different. Owing to the post-cross-linking effect all decrease after ageing. The cross-link density of composites increasing considerably can lead to a decrease of all the elongation at break, especially for NM-0.5 and NM-2.0 composites.

3.3. Micromorphology of composites by SEM: Tensile fractured surface for composites is characterised by SEM images to analyse this significant improvement in mechanical properties. SEM images of (a), (b), (c), (d) and (e) in Fig. 3 stand for NM-0,

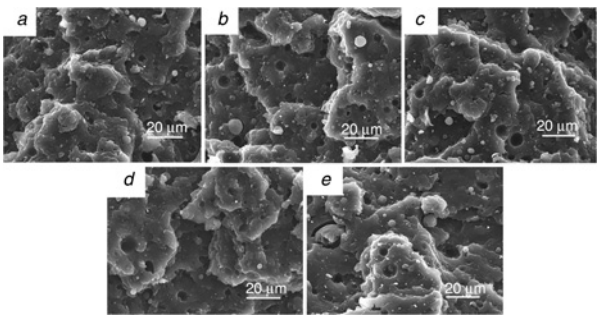

Fig. 3 *SEM images of tensile fractured surfaces of composites*
a NM-0
b NM-0.5
c NM-1.0
d NM-1.5
e NM-2.0

Table 5 Bound rubber content and filler–rubber interaction of NR compounds

MWNTs/CB ratio	0/40	0.5/39.5	1.0/39	1.5/38.5	2.0/38
Rb, %	40.61	46.14	50.00	49.20	48.06
Q_f/Q_g	0.61	0.43	0.41	0.59	0.56

Table 6 Heat build-up and compression set of NR/CB composites

MWNTs/CB ratio	0/40	0.5/39.5	1.0/39	1.5/38.5	2.0/38
heat build-up, °C	11.4	9.4	9.6	10.3	10.1
compression set, %	6.2	1.7	1.8	1.5	1.4

NM-0.5, NM-1.0, NM-1.5 and NM-2.0, respectively. As shown in Fig. 3, it is obvious that the surface for composites with MWNTs is much rougher with many protuberances than that of CB-filled composites. It maybe due to the stronger interaction among MWNTs, CB, NR and better dispersity as mentioned earlier which makes the fracture surface of the sample much rougher. Moreover, the increase of mechanical properties of composites with MWNTs due to stronger filler–rubber interaction and the more bound rubber, as shown in Table 5.

3.4. Heat build-up: Heat build-up of all composites is compared in Table 6. The results show that heat build-up decreases when CB is replaced by MWNTs and the corresponding compression set decreases more obviously. For instance, both NM-0.5 and NM-1.0 composites show the lower heat build-up; meanwhile, compression set are smaller. It is attributed to better dispersity and strong filler–rubber interaction. The results suggest that the combination of latex co-precipitation masterbatch and mechanical blending method is very practical to prepare composites with lower heat build-up and compression set.

In addition, effective elasticity and hysteresis loss of all the composites is shown in Table 7. The results show that effective elasticity increase when CB is partially replaced by MWNTs and the corresponding hysteresis loss decrease. However, effective elasticity decreases when the concentration of MWNTs is up to 2.0 phr while corresponding hysteresis loss increases during to worst dispersity.

3.5. Dynamic properties: Many factors such as rubber network properties, filler–rubber interaction and strong filler–filler interaction govern the relationship between the shear strain and storage modulus of vulcanisates as reported. However, at small strains, the increased storage modulus mainly depends on the increased strong filler–filler interaction. Therefore, in order to study the filler network structure, we always investigate the relationship of storage modulus and shear strain. As shown in Fig. 4, Fig. 4*a* shows the relationship of G' and strain of compounds and Fig. 4*b* represents tan δ of compounds, respectively. The dynamic viscoelastic properties have strain dependence and regarding as storage modulus is called the Payne effect [23–25] in a filled rubber compound. When the filler network structure is weaker in rubber matrix indicates the lower

Table 7 Effective elasticity and hysteresis loss ratio of composites

MWNTs/CB ratio	0/40	0.5/39.5	1.0/39	1.5/38.5	2.0/38
effective elasticity, %	71.53	72.73	75.86	74.40	61.38
hysteresis loss, %	28.47	27.27	24.14	25.60	38.62

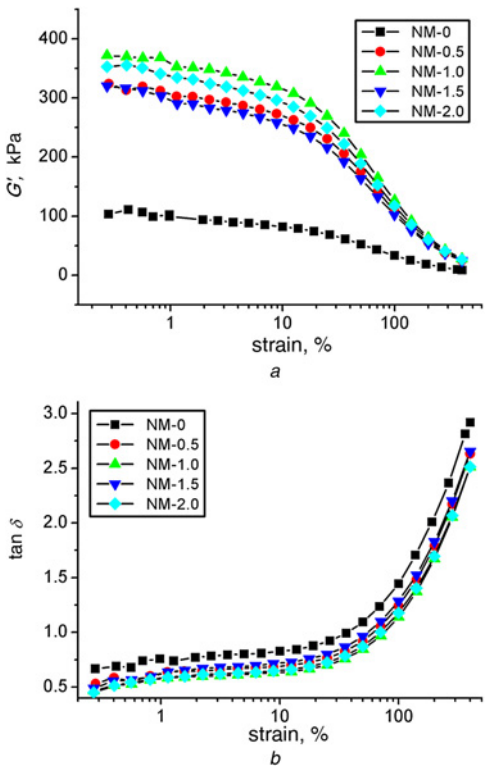

Fig. 4 *Curves of G′ and tan δ against strain of compounds*
a G' against strain of compounds
b tan δ against strain of compounds

Payne effect and the higher uniformity of the filler dispersion. Fig. 4*a* shows when CB is partially replaced by MWNTs composites exhibit obvious Payne effect, especially NM-1.0 composites show the highest Payne effect. In general, when the fillers are better dispersed, a rubber matrix shows a lower Payne effect. For example, adding a silane coupling agent to a silica-filled system leads to a decrease of the Payne effect as the expense of the filler–filler interaction [26] developed by the rubber–filler interaction. However, when the agglomerates are dispersed into individual tubes the filler–filler interaction increases because of extremely high anisotropic character of MWNTs, as an interconnecting network throughout the matrix was formed. Subramaniam *et al.* [27] observed that the well-dispersed tubes present strong Payne effect but worst dispersed tubes yield little effect on the strain dependence of the modulus, and proposed this mechanism. Within the small strain (<10%), the platform suggested that well-developed three-dimensional filler network was formed and G' is mainly decided by the interaction between filler and filler. When the strain is more than 10%, G' is mainly decided by the interaction between filler and rubber. At all strains, the MWNT added composites show 3–4 times larger G' than non-MWNT added composites, so that authors attribute the improvement of the mechanical properties with the addition of MWNT to the stronger interactions between MWNTs, CB and rubber and better dispersity.

Fig. 4*b* shows when CB is partially replaced by MWNTs, compounds exhibit smaller tan δ. It is attributed to more bound rubber and stronger filler–rubber interaction as mentioned above. As we all know, in composites, polymer chains are trapped and absorbed on the filler surfaces that will confine the mobility and flexibility of chains [28–30]. The dispersion of fillers and the interfacial interaction between the polymer matrix and the fillers primarily governed the extent of the confinement.

Fig. 5 shows the enlightening dynamic mechanical against temperature spectra for composites. Below the glass transition

doi: 10.1049/mnl.2016.0003

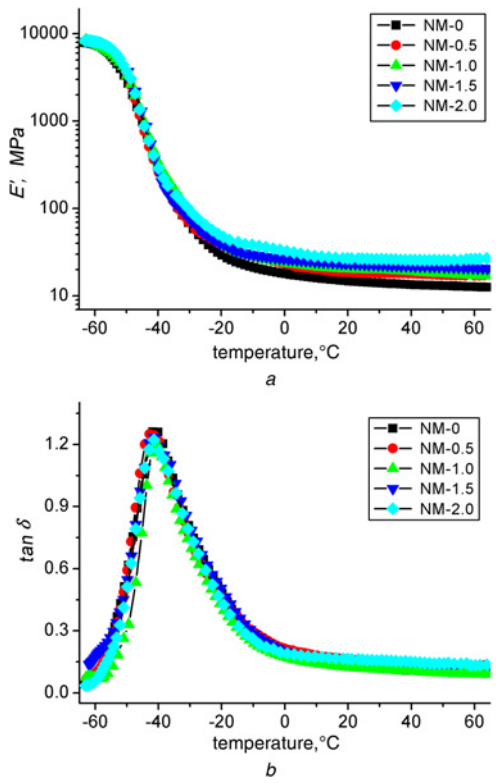

Fig. 5 *Curves of E′ and tan δ against temperature for vulcanisates*
a E' against temperature for vulcanisates
b tan δ against temperature for vulcanisates

temperature, from Fig. 5*a*, it can be observed that composites with MWNTs show the larger modulus compared with that of CB-filled composites. We can observe that adding MWNTs to the compounds increases the E' values within the rubbery plateau area and makes the material stiffer. Actually, the segmental motion was frozen in the low-temperature domain and the storage modulus was mainly attributed to the filler–filler interaction. According to Fig. 5*a*, the dynamic behaviour within this strain belongs to linear behaviour when the strain is <10%. On the contrary, the storage modulus was attributed to both the rubber–filler interaction and larger filler volume fraction as the temperature was ambient temperature or above. In higher temperature, the NM-2.0 composites presented higher modulus compared with other composites.

From Fig. 5*b* we can observe, at glass transition temperature, a decrement in intensity of tan δ of composites filled by MWNTs. Internal kinetic friction for composites is inversely proportional to interfacial interaction between fillers and polymer matrix, and energy dissipation always can be shown by the peak value of tan δ. On the other hand, tan δ for NM-1.0 composites shows much lower tan δ which is good to rolling resistance property in the higher-temperature zone (20–65°C). The main reason for the lowest tan δ of NM-1.0 composites is the better dispersity and stronger filler–rubber interaction provoked higher elasticity.

4. Conclusions: Effect of replacing CB by MWNTs on the performance and structure of NR/CB composites was studied in this Letter. Compared with NR/CB composites, NM presents better filler dispersity and dynamic properties of the MWNT up to a certain concentration. For instance, sample with 1 phr MWNTs shows obviously the highest tensile strength, 28.60 MPa, and almost the lowest heat build-up, only 9.6°C, and it is attributed to that not only large cross-link density and better filler dispersity but also high effective elasticity and large filler–rubber interaction. Payne effect increased when CB was partially replaced by MWNTs. Badly dispersed tubes gave little effect on dependence of the modulus and strain, whereas well-dispersed tubes yielded strong Payne effect. At a higher concentration, MWNTs tended to aggregate and was not conducive to improve dynamic properties or even deteriorate the properties of composites, e.g. NM-2.0 composites show low tear strength and large hysteresis loss.

5. Acknowledgment: This research was supported by the National Science Foundation of China (grant no. 51275265).

6 References

[1] Pal K., Rajasekar R., Kang D.J., *ET AL.*: 'Effect of fillers on natural rubber/high styrene rubber blends with nanosilica: morphology and wear', *Mater. Des.*, 2010, **31**, p. 677
[2] Claiden P., Knowles G., Liu F., *ET AL.*: 'Modelling of nano-filler reinforcement, filler strength and experimental results of nanosilica composites made by a precipitation method', *Comput. Mater. Sci.*, 2014, **94**, p. 27
[3] Heinrich G., Kluppel M., Vilgis T.A.: 'Reinforcement of elastomers', *Curr. Opin. Solid State Mater.*, 2002, **6**, p. 195
[4] Gotz C., Lim G.T., Puskas J.E., *ET AL.*: 'Investigation of structure-property relationships of polyisobutylene-based biomaterials: morphology, thermal, quasi-static tensile and long-term dynamic fatigue behavior', *J. Mech. Behav. Biomed.*, 2012, **10**, p. 206
[5] Dong B., Liu C., Lu Y.L., *ET AL.*: 'Synergistic effects of carbon nanotubes and carbon black on the fracture and fatigue resistance of natural rubber composites', *J. Appl. Polym. Sci.*, 2015, **132**, pp. 995–1005
[6] Poikelisp M., Das A., Dierkes W., *ET AL.*: 'The effect of partial replacement of carbon black by carbon nanotubes on the properties of natural rubber/butadiene rubber compound', *J. Appl. Polym. Sci.*, 2013, **130**, p. 3153
[7] Yang G.W., Liao Z.F., Yang Z.J., *ET AL.*: 'Effects of substitution for carbon black with graphene oxide or graphene on the morphology and performance of natural rubber/carbon black composites', *J. Appl. Polym. Sci.*, 2015, **132**, 41832(1–9)
[8] Jiang H.X., Ni Q.Q., Natsuki T.: 'Effect of carbon nanotubes on the properties of natural rubber composites', *Key Eng. Mater.*, 2011, **464**, p. 660
[9] Bokobza L.: 'Enhanced electrical and mechanical properties of multiwall carbon nanotube rubber composites', *Polym. Adv. Technol.*, 2012, **23**, p. 1543
[10] Zhou X., Zhu Y., Liang J., *ET AL.*: 'New fabrication and mechanical properties of styrene–butadiene rubber/carbon nanotubes nanocomposite', *J. Mater. Sci. Technol.*, 2010, **26**, p. 1127
[11] De Falco A., Goyanes S., Rubiolo H., *ET AL.*: 'Carbon nanotubes as reinforcement of styrene–butadiene rubber', *Appl. Surf. Sci.*, 2007, **254**, p. 262
[12] Sui G., Zhong W.H., Yang X.P., *ET AL.*: 'Preparation and properties of natural rubber composites reinforced with pretreated carbon nanotubes', *Polym. Adv. Technol.*, 2008, **19**, p. 1543
[13] Shanmugharaj A.M., Bae J.H., Lee K.Y., *ET AL.*: 'Physical and chemical characteristics of multiwalled carbon nanotubes functionalized with aminosilane and its influence on the properties of natural rubber composites', *Compos. Sci. Technol.*, 2007, **67**, p. 1813
[14] Bokobza L., Rahmani M., Belin C., *ET AL.*: 'Blends of carbon blacks and multiwall carbon nanotubes as reinforcing fillers for hydrocarbon rubbers', *J. Polym. Sci.*, 2008, **46**, pp. 1939
[15] Xu C.H., Chen Y.K., Wang Y.P., *ET AL.*: 'Temperature dependence of the mechanical properties and the inner structures of natural rubber reinforced by in situ polymerization of zinc dimethacrylate', *J. Appl. Polym. Sci.*, 2013, **128**, p. 2350
[16] Singh A.: 'Synthesis and applications of polyacrylamide gels catalyzed by silver nitrate', *J. Appl. Polym. Sci.*, 2011, **119**, p. 1084
[17] Sirousazar M., Kokabi M., Hassan Z.M.: 'Swelling behavior and structural characteristics of polyvinyl alcohol/montmorillonite nanocomposite hydrogels', *J. Appl. Polym. Sci.*, 2012, **123**, p. 50
[18] Johns J., Rao V.: 'Characterization of natural rubber latex/chitosan blends', *Int. J. Polym. Anal. Charact.*, 2008, **13**, p. 280
[19] Mao Y.Y., Wen S.P., Chen Y.L., *ET AL.*: 'High performance graphene oxide based rubber composites', *Sci. Rep., UK*, 2013, **3**, p. 1
[20] Qu L.L., Yu G.Z., Wang L.L., *ET AL.*: 'Effect of filler–elastomer interactions on the mechanical and nonlinear viscoelastic behaviors of chemically modified silica-reinforced solution-polymerized styrene butadiene rubber', *J. Appl. Polym. Sci.*, 2012, **126**, p. 116

[21] Lorenz O., Parks C.R.: 'The crosslinking efficiency of some vulcanizing agents in natural rubber', *J. Polym. Sci.*, 1961, **50**, p. 299
[22] Darwish N.A., Shehata A.B., Abd El-Megeed A.A., *ET AL.*: 'Compatibilization of SBR/NBR blends using poly acrylonitrile as compatibilizer', *Polym. Plast. Technol. Eng.*, 2005, **44**, p. 1297
[23] Sorokin V.V., Ecker E., Stepanov V.G., *ET AL.*: 'Experimental study of the magnetic field enhanced Payne effect in magnetorheological elastomers', *Soft Matter*, 2014, **10**, p. 8765
[24] Luginsland H.D., Frohlich J., Wehmeier A.: 'Influence of different silanes on the reinforcement of silica-filled rubber compounds', *Rubber Chem. Technol.*, 2002, **75**, p. 563
[25] Li Y., Han B.Y., Wen S.P., *ET AL.*: 'Effect of the temperature on surface modification of silica and properties of modified silica filled rubber composites', *Compos. A*, 2014, **62**, p. 52
[26] Reuvekamp L.A.E.M., ten Brinke J.W., van Swaaij P.J., *ET AL.*: 'Effects of time and temperature on the reaction of TESPT silane coupling agent during mixing with silica filler and tire rubber', *Rubber Chem. Technol.*, 2002, **75**, p. 187
[27] Subramaniam K., Das A., Steinhauser D., *ET AL.*: 'Effect of ionic liquid on dielectric, mechanical and dynamic mechanical properties of multi-walled carbon nanotubes/polychloroprene rubber composites', *Eur. Polym. J.*, 2011, **47**, p. 2234
[28] Wu S.W., Tang Z.H., Guo B.C., *ET AL.*: 'Effects of interfacial interaction on chain dynamics of rubber/graphene oxide hybrids: a dielectric relaxation spectroscopy study', *RSC Adv.*, 2013, **3**, p. 14549
[29] Zhang H., Zhang Z.Y., Zhao G.Z., *ET AL.*: 'Influence of fillers on semi-efficient vulcanized natural rubber: dynamic properties and heat buildup', *Rubber Chem. Technol.*, 2015, **88**, p. 412
[30] Liu J., Wu Y., Shen J.X., *ET AL.*: 'Polymer-nanoparticle interfacial behavior revisited: a molecular dynamics study', *Phys. Chem. Chem. Phys.*, 2011, **13**, p. 13058

doi: 10.1049/mnl.2016.0003